

Molecular-orbital- K -vacancy production by direct impact in symmetric heavy-ion collisions*

Walter R. Thorson

Department of Chemistry, University of Alberta, Edmonton, Alberta, Canada

(Received 9 December 1974; revised manuscript received 24 February 1975)

Using simple scaling laws based on the adiabatic approximation, Meyerhof and co-workers have compared experimental data on K -vacancy production cross sections for symmetric collisions of heavy atoms and ions, with *ab initio* calculations of cross sections for direct impact ionization of hydrogen atoms by slow protons, done in this laboratory. It is shown here that the relative magnitudes and energy dependences of such cross sections can be understood using a simplified model theory; dominant features are determined by the oscillatory exponential factors associated with momentum and energy loss by the heavy particles, rather than the electronic-coupling matrix elements.

I. INTRODUCTION

In recent papers Meyerhof and co-workers¹⁻³ have compared experimental data for K -vacancy production in symmetric and near-symmetric heavy-ion collisions with *ab initio* calculations, done in this laboratory,⁴⁻⁶ of cross sections for direct impact ionization of hydrogen atoms by slow protons. A simple Z -scaling law based on the adiabatic approximation (neglecting electron-electron interactions) is used.⁷ The experimental vacancy-production cross sections are about an order of magnitude larger than the calculated ionization cross sections; however, the most important result of the H_2^+ calculations, viz., that the ionization cross section for the $2p\sigma_u$ electron is about 500 times larger than that for the $1s\sigma_g$ electron, is confirmed by the experimental data. For symmetric collisions ($Z_1 \approx Z_2$), Meyerhof *et al.*³ found that an empirical scaling law can account for both the $2p\sigma_u$ and $1s\sigma_g$ direct ejection processes with a single form, i.e.,

$$Z^2\sigma_K = F(E_1 m / GM_1), \quad (1)$$

where Z is the (mean) nuclear charge, E_1 and M_1 the projectile lab energy and mass, and G the electronic binding energy of the apposite molecular orbital at the distance of closest approach. They noted, however, that Eq. (1) lacked a theoretical basis.

According to Eq. (1) any difference between $2p\sigma_u$ and $1s\sigma_g$ cross sections is due to the greater relative binding energy of the $1s\sigma_g$ electron. This suggests that a theoretical explanation of Eq. (1) will be found in the rapidly oscillating factor representing effects of momentum and energy loss by the heavy particles, rather than in any details associated with electronic matrix elements, radial or angular coupling, etc. We show here that this is indeed the case. In our paper⁶ reporting the exact calculations for H_2^+ it was suggested that angular

coupling specifically is the dominant contributor to direct impact ionization from the $2p\sigma_u$ orbital; this suggestion is misleading and incorrect. As a result of the model calculations done here we conclude that K -vacancy-production cross sections associated with direct impact ionization by heavy particles contain little information about the character of electronic-coupling matrix elements, and are mainly determined by the factors associated with the heavy-particle energy loss.

More recent studies⁸ on K -vacancy production in *asymmetric* heavy-ion collisions do not fit Eq. (1) without modification, and different scaling laws seem to result for the $1s\sigma_g$ and $2p\sigma_u$ excitation processes. In this model study we restrict ourselves entirely to the *symmetric* case, and we do not consider relativistic effects, as is appropriate for H_2^+ . By making a number of simplifying assumptions, we can deduce Eq. (1), including approximately the quantitative form of F , from the *ab initio* theory of Refs. 4-6; however, it appears that the success of Eq. (1) in fitting the magnitudes of both $2p\sigma_u$ and $1s\sigma_g$ cross sections may be fortuitous.

It is a bit surprising from a theoretical viewpoint that the data for heavy-ion systems can be compared even semiquantitatively with Z -scaled H_2^+ results. While the bound $1s\sigma_g$ and $2p\sigma_u$ orbitals of the heavy-ion systems are much like those of a Z -scaled H_2^+ , the continuum states are quite different due to screening by other electrons, so electronic matrix elements for ionization in the two systems need not be comparable. Also, the total K -vacancy production rate includes transitions to vacant excited bound orbitals, in addition to ionization. The behavior of the cloud of outer electrons cannot be adiabatic,⁴ and this further complicates the dynamics of the system. If there is an initial L -shell vacancy in one of the ions, the strong $2p\sigma_u$ - $2p\pi_u$ angular coupling is the dominant contributor to K -vacancy production,⁹ and the di-

rect-impact processes are only of interest because this route is assumed to be closed by the Pauli exclusion principle, the L -shell levels being filled. Since (as we will show here) the ionization energy of an electron has a dominant effect on the efficiency of a direct ionization process, it is possible in a single collision that second-order processes, initial L -vacancy creation followed by $2p\sigma_u$ - $2p\pi_u$ strong coupling, can significantly enhance the $2p\sigma_u$ vacancy production¹⁰; the data of Meyerhof¹ show such an enhancement of $2p\sigma_u$ over $1s\sigma_g$ when compared to the $2p\sigma_u/1s\sigma_g$ ionization cross-section ratio computed for scaled H_2^+ . In a pessimistic view, one can say that the only real agreement between the observations of Meyerhof and co-workers on K -vacancy production in heavy ions, and our calculated ionization cross sections for scaled H_2^+ orbitals, is the σ_u/σ_g cross section ratio of about 500 and (less accurately) the approximate E dependence. Since it is shown here that these features do not reflect electronic matrix-element structure but are effects of nonresonant momentum and energy transfer from heavy particles to electron, it could be argued that there is no *a priori* reason to expect good agreement on absolute magnitudes; principles governing relative magnitudes and energy dependence are the same in the two cases but the electronic matrix elements may be quite different. But even if the H_2^+ system is a model for K -vacancy production only in this limited sense, the results still have useful bearing on the interpretation of experimental data. We present them in that conservative context, rather than the more speculative one of a direct congruence.

II. MODEL THEORY

The direct-impact ionization cross section for relative collision energy E and ejected electron energy ϵ is given by^{4,6}

$$\sigma(E, \epsilon) = 2\pi \int_0^\infty b db P(E, \epsilon; b) \quad (2)$$

and the ionization probability per collision of impact parameter b can be divided into electronic partial-wave components,

$$P(E, \epsilon; b) = \sum_{L, M_L} |C^+(\epsilon LM_L; E, b)|^2, \quad (3)$$

where the trajectory integrals $C^+(\epsilon LM_L; E, b)$,

$$C^+(\epsilon LM_L; E, b) = \int_{-\infty}^{\infty} dt \dot{a}(\epsilon LM_L; E, b; t), \quad (4)$$

are evaluated along the appropriate classical trajectory for E, b, L . For symmetric systems, parity separation into g and u parts (parity of L) can be made. Equations (12)–(17) of Ref. 6 give rigor-

ous expressions for the amplitudes $\dot{a}(\epsilon LM_L)$. In general these are composed of terms of the form

$$\dot{a} = (\dot{R}T_R + \dot{\theta}T_\theta)e^{i\Delta(t)}, \quad (5)$$

where \dot{R} , $\dot{\theta}$ are radial and angular nuclear velocities and T_R , T_θ the associated radial and angular “nonadiabatic” coupling matrix elements. The exponent $\Delta(t)$ is given by

$$\Delta(t) = \int_0^t [\epsilon - \epsilon_i(t')] dt', \quad (6)$$

where $\epsilon_i(t')$ is the adiabatic electronic energy of the initial state i which is coupled to the continuum via the elements T . The rapid oscillation of the exponential represents the effect of energy/momentum transfer on the heavy-particle motion and has a strong influence on the ionization probability.

To obtain a simple model we make several approximations.

1. *Drop $2p\pi_u$ terms.* In H^+ - H collisions, strong-coupled excitation of the $2p\pi_u$ state is an important process,¹¹ and the contribution to *direct ionization* from the level so excited is significant. However, we neglect it here. (It is worth noting that in spite of this our resulting predictions for the u ionization agree well with the exact H_2^+ calculations.) As pointed out in the Introduction, the $2p\pi_u$ level is *occupied* in the many-electron heavy-ion systems, so (in zero order) ignoring all coupling to the $2p\pi_u$ level may be even more appropriate there than for H_2^+ .

2. *Neglect all but the largest coupling matrix elements.* The dominant matrix elements between molecular bound levels and molecular continuum states are as follows:

$$\begin{aligned} T_{00} &= \langle \epsilon s\sigma_g | H'_R | 1s\sigma_g \rangle: \text{“s-wave” radial} \\ &\quad \sigma_g \rightarrow \sigma_g \text{ coupling;} \\ T_{10} &= \langle \epsilon p\sigma_u | H'_R | 2p\sigma_u \rangle: \text{“p-wave” radial} \\ &\quad \sigma_u \rightarrow \sigma_u \text{ coupling;} \\ T_{11} &= \langle \epsilon p\pi_u | H'_\theta | 2p\sigma_u \rangle: \text{“p-wave” angular} \\ &\quad \sigma_u \rightarrow \pi_u \text{ coupling;} \\ T_{30} &= \langle \epsilon f\sigma_u | H'_R | 2p\sigma_u \rangle: \text{“f-wave” radial} \\ &\quad \sigma_u \rightarrow \sigma_u \text{ coupling.} \end{aligned}$$

Although T_{30} is not really negligible compared to T_{10} or T_{11} , we have also neglected it for simplicity. The three matrix elements retained are described by simple analytical approximations:

$$\begin{aligned} T_{00}(R) &= A_0(\epsilon)R \exp[-\alpha_0(\epsilon)R], \\ T_{10}(R) &= A_1(\epsilon)R[a_1(\epsilon) - R] \exp[-\alpha_1^2(\epsilon)R^2], \\ T_{11}(R) &= A_\pi(\epsilon)R^2 \exp[-\alpha_\pi^2(\epsilon)R^2]; \end{aligned} \quad (7)$$

while it is the case that Gaussian forms fit the u

elements best, and an exponential form fits the g element best, no special significance should be given to that fact.¹² Table I gives approximate ϵ dependences of the parameters in (7), but the effect of replacing them by suitable constant values is not great.

3. *Ignore mixing and interference effects due to nonspherical molecular symmetry.* This means that the waves designated s and p above are treated as if they were angular-momentum eigenstates, and also the variation of electronic-scattering phase shifts with R is neglected. However, the quantum numbers $\Lambda = 1, 0$ in $T_{L\Lambda}$ above refer to the molecular axis, and to obtain amplitudes associated with lab axes (L, M_L), the factors $d_{\Lambda M_L}^{(L)}(\theta)$ appearing in the exact expressions⁴⁻⁶ must be retained.

4. *Coulomb trajectories.* A simpler assumption, of course, would be to use constant-velocity straight-line paths. However, for angular coupling certain singularities arise in the integrals, and it is well known that in the $2p\sigma_u - 2p\pi_u$ strong-coupling problem the results for Coulomb trajectories differ greatly from those for straight lines.¹¹ More surprising, we also find here that even for the σ_g case (where only radial coupling occurs), the straight-line path gives a different E dependence to the total cross section from that obtained using Coulomb trajectories (see Sec. IIIB below).

5. *Compute $\Delta(t)$ assuming essentially constant energy gaps, $\epsilon - \epsilon_i$.* This is certainly not valid for the σ_g case, as the results show, but it permits analytical evaluation of integrals.

With these assumptions we can obtain analytical expressions for trajectory integrals $C^+(\epsilon LM_L)$, which are nonzero only for $L=0, M=0$ (σ_g case) and $L=1, M_L=0, \pm 1$ (σ_u case). They are given by

$$C^+(\epsilon 00) = J_{00}(\epsilon; E, b) = - \int_{-\infty}^{\infty} dt \dot{R}(t) T_{00}[R(t)] e^{i\Delta_g(t)}, \quad (8a)$$

where

$$\Delta_g(t) = \int_0^t dt' \{ \epsilon - \epsilon_{1s\sigma_g}[R(t')] \} = [\epsilon - \bar{\epsilon}_{1s\sigma_g}] t; \quad (8b)$$

$$C^+(\epsilon 10) = J_{10}^{\text{rad}}(\epsilon; E, b) + J_{10}^{\text{ang}}(\epsilon; E, b), \quad (9a)$$

$$C^+(\epsilon 1, \pm 1) = J_{11}^{\text{rad}}(\epsilon; E, b) + J_{11}^{\text{ang}}(\epsilon; E, b), \quad (9b)$$

where

$$J_{10}^{\text{rad}} = - \int_{-\infty}^{\infty} \dot{R} dt e^{i\Delta_u(t)} \cos \theta(t) T_{10}[R(t)], \quad (10a)$$

$L=0, M=0$ (σ_g case)

$$J_{00}(\epsilon, v, b) = -A_0 c^2 e^{-\omega} \left\{ \int_{-\infty}^{\infty} dz [1 + D/(1+z^2)^{1/2}] \exp[i\xi z - \tau(1+z^2)^{1/2}] \right\}. \quad (12)$$

TABLE I. Energy dependence of matrix-element parameters (ϵ is continuum energy in a.u.).

$A_0(\epsilon) = 0.50$ (const)
$\alpha_0(\epsilon) = 2.890 - 2.222/(\epsilon + 1.5)$
$A_1(\epsilon) = 0.0208 + 0.062/(\epsilon + 0.5)$
$a_1(\epsilon) = 1.633 + 0.40/(\epsilon + 0.5)$
$\alpha_1(\epsilon) = 0.50 - 0.070/(\epsilon + 0.5)$
$A_\pi(\epsilon) = 0.033 + 0.073/(\epsilon + 0.5)$
$\alpha_\pi(\epsilon) = 0.30 + 0.18/(\epsilon + 0.5)$

$$J_{11}^{\text{rad}} = -2^{-1/2} \int_{-\infty}^{\infty} \dot{R} dt e^{i\Delta_u(t)} \sin \theta(t) T_{10}[R(t)], \quad (10b)$$

$$J_{10}^{\text{ang}} = 2^{1/2} \int_{-\infty}^{\infty} \dot{\theta} dt e^{i\Delta_u(t)} \sin \theta(t) T_{11}[R(t)], \quad (10c)$$

$$J_{11}^{\text{ang}} = \int_{-\infty}^{\infty} \dot{\theta} dt e^{i\Delta_u(t)} \cos \theta(t) T_{11}[R(t)], \quad (10d)$$

and

$$\Delta_u(t) = \int_0^t \{ \epsilon - \epsilon_{2p\sigma_u}[R(t')] \} dt' = (\epsilon - \bar{\epsilon}_{2p\sigma_u}) t. \quad (10e)$$

[In (10e) and (8b) $t'=0$ corresponds to the turning point.]

Define the Coulomb parameter $\eta = Z^2/2Eb = Z^2/Mv^2b$, where M is the heavy-particle reduced mass and v the incident relative velocity (all in a.u.). Assuming constant energy gaps, $\Delta\epsilon = (\epsilon - \epsilon_i)$, $\Delta(t)$ can be evaluated exactly,

$$\Delta(t) = (\pm)(\Delta\epsilon/v) \{ (u^2 - c^2)^{1/2} + \eta b \ln[(u/c) + (u^2 - c^2)^{1/2}/c] \}, \quad (11)$$

where $c = b(1 + \eta^2)^{1/2}$, $u = R - \eta b$, $u(0) = c$. We can approximate (11) by its first term alone, since the approximation that $\Delta\epsilon$ is constant is even less accurate.

The trajectory integrals (10a)–(10d) and (8a) are evaluated by changing the independent variable from t to $z = (u^2 - c^2)^{1/2}/c$, where the branch cut is chosen so that z changes sign on the real axis. It is convenient to define parameters

$$\beta = (\Delta\epsilon/v), \quad D = \eta b/c, \quad \xi = \beta c,$$

$$\tau = \alpha c, \quad \xi = (\xi^2 + \tau^2)^{1/2}, \quad \omega = \tau D = \alpha Z^2/2E,$$

$$x = (\xi/\tau) = (\beta/\alpha),$$

and $\alpha = \alpha_0, \alpha_1$, or α_π as required. Then the trajectory integrals are as follows:

$L=1, M=0, \pm 1$ (σ_u case)

$$\begin{aligned} J_{10}^{\text{rad}} &= -A_1 c^2 e^{-\omega^2 - \tau^2} \{ (1 - D^2) [(a_1 - cD)G_{2u} - cG_{5u}] + D[(a_1 - cD)G_{1u} + D(a_1 - cD)G_{4u} - cG_{4u} - cDG_{6u}] \}, \\ J_{11}^{\text{rad}} &= -[A_1 c^2 (1 - D^2)^{1/2} / 2^{1/2}] e^{-\omega^2 - \tau^2} \{ D[(a_1 - cD)G_{2u} - cG_{5u}] + [(a_1 - cD)G_{1u} + D(a_1 - cD)G_{4u} - cG_{4u} - cDG_{6u}] \}, \\ J_{10}^{\text{ang}} &= -2^{1/2} A_\pi (1 - D^2) c^2 e^{-\omega^2 - \tau^2} \{ [G_{0u} + DG_{3u}] + DG_{1u} \}, \\ J_{11}^{\text{ang}} &= A_\pi (1 - D^2)^{1/2} c^2 e^{-\omega^2 - \tau^2} \{ D[G_{0u} + DG_{3u}] - G_{1u} \}, \end{aligned} \quad (13)$$

where the basic integrals $G_{nu}(\omega, x, \tau)$ are defined by

$$G_{nu}(\omega, x, \tau) = \int_{-\infty}^{\infty} dz (1 + z^2)^{-1/2} \exp[i\xi z - \tau^2 z^2 - 2\omega\tau(1 + z^2)^{1/2}] f_{nu}(z), \quad (14a)$$

with

$$\begin{aligned} f_{0u} &= 1, \quad f_{1u} = z, \quad f_{2u} = z^2, \quad f_{3u} = (1 + z^2)^{1/2}, \\ f_{4u} &= z(1 + z^2)^{1/2}, \quad f_{5u} = z^2(1 + z^2)^{1/2}, \quad f_{6u} = z(1 + z^2). \end{aligned} \quad (14b)$$

The σ_g integrals can be done in closed form¹³:

$$\begin{aligned} J_{00}(\epsilon, v, b) &= -8iA_0 e^{-\omega} [\alpha\beta / (\alpha^2 + \beta^2)^2] \\ &\quad \times \{ \bar{K}_2(\xi) + (\omega/2)(1 + x^2)\bar{K}_1(\xi) \}, \end{aligned} \quad (15)$$

where $\bar{K}_n(\xi) = (\frac{1}{2}\xi)^n K_n(\xi)$, and $K_n(\xi)$ is the modified Bessel function of second kind.

The basic σ_u integrals G_{nu} are not quite so easy to evaluate. The stationary-phase result is valid if $\tau \gg 2x$, giving the result

$$\begin{aligned} G_{0u} &= \{ \pi / \tau(\tau + \omega) [1 - x^2 / 4(\tau + \omega)^2] \}^{1/2} \\ &\quad \times \exp[-(\xi^2 / 4\tau(\tau + \omega)) - 2\omega\tau], \end{aligned} \quad (16a)$$

but this is valid only when the relative magnitudes of the G_{nu} integrals are negligible (large b). For $x \geq 10$ and $\tau \leq \frac{1}{4}x$,

$$\begin{aligned} e^{-\tau^2} G_{0u}(\omega, x, \tau) &= 2 \sum_{m=0}^{\infty} \sum_{n=0}^{\infty} \left(\frac{(-1)^m (2m + 2n)!}{n! 2m! (n+m)!} \right) \\ &\quad \times \left(\frac{\tau}{2x} \right)^n \left(\frac{2\omega^2 \tau}{x} \right)^m K_{m+n}(x\tau); \end{aligned} \quad (16b)$$

this is an asymptotic expansion.¹⁴ For $x \geq 10$ and $\tau \geq \frac{1}{4}x$ the integrals G_{nu} are again relatively negligible; and for $x < 10$ a method of numerical Fourier quadrature is most efficient. (For the energies E of interest, $E \leq 500$ eV, and values of ϵ for which cross sections are significant, $x \geq 4.0$.) G_{nu} are obtained from (16b) by differentiations with respect to ω and x .

III. RESULTS OF CALCULATIONS

From the trajectory integrals $C^+(\epsilon LM_L; E, b)$ the ionization probabilities $P_g(\epsilon, E; b)$, $P_u(\epsilon, E; b)$ and

corresponding differential cross sections $\sigma_g(E; \epsilon)$, $\sigma_u(E; \epsilon)$ can be calculated by Eqs. (2) and (3). Total cross sections are given by

$$\sigma_g(E) = \int_0^{\infty} d\epsilon \sigma_g(E; \epsilon) \quad (17)$$

and similarly for $\sigma_u(E)$.

Since $K_n(\xi) \sim e^{-\xi}$ for large ξ , and ξ is dominated by ξ when $\beta \gg \alpha$, decreasing the wavelength of the oscillatory factor in (5) has a strongly damping effect. As $\beta = (\Delta\epsilon/V)$ increases, the contribution for a given impact parameter decreases exponentially, not with α , as might have been expected, but with β .

A. Z-scaling laws

Scaling laws which permit data for different Z values to be placed on a common curve can be deduced on quite general grounds (from the formal theory of the adiabatic approximation),⁷ but it is useful to see how they emerge here.

For H_2^+ -like (one-electron) systems with nuclear charges Z , the parameters of Eq. (7) scale as follows: $A_0, \alpha_0, A_\pi, \alpha_\pi, \alpha_1 \sim Z^{+1}, A_1 \sim Z^{+2}, a_1 \sim Z^{-1}$. All characteristic distances are scaled as Z^{-1} , all velocities (including collision velocity) as Z^{+1} , energies as Z^{+2} . The reduced mass M , which appears in ω , scales approximately as Z^{+1} .¹⁵ Then the parameters $\tau, \xi, \zeta, \omega, D, x$, etc., are scale invariant, and the scaling properties of $P(E, \epsilon; b)$, $\sigma(E; \epsilon)$, and $\sigma(E)$ can be deduced immediately from Eqs. (12) and (13). In particular, $P(E, \epsilon; b)$ scales as Z^{-2} , $\sigma(E, \epsilon)$ as Z^{-4} , and $\sigma(E)$ as Z^{-2} . The probability $P(E; b)$ of ionization per collision (of scaled E, b) is *invariant*. This invariance results quite generally from the fact that the system Hamiltonian is homogeneous of degree 2 in Z and that its time dependence is scaled commensurately with its eigenfrequencies (by scaling collision velocity as Z^{+1}). For asymmetric collisions ($Z_1 \neq Z_2$) this homogeneity is destroyed.

B. Approximate energy dependence

Using Eq. (15), a rough derivation of the dependence of the σ_g cross section on collision energy and ionization energy can be given. In this connection it is of interest to obtain first the result using straight-line trajectories, and then for Coulomb trajectories; we shall see that they are qualitatively different.

1. For straight-line trajectories

The result for $C^+(\epsilon 00)$ is given by Eq. (15), provided we write $c=b$ everywhere and set $\omega=0$. Then we have

$$P_g(E, \epsilon; b) = 64A_0^2 [\alpha^2 \beta^2 / (\alpha^2 + \beta^2)^4] [\bar{K}_2(\xi)]^2 \quad (18a)$$

and the differential cross section is

$$\sigma_g(E; \epsilon) = (256\pi A_0^2 / 5) [\alpha^2 \beta^2 / (\alpha^2 + \beta^2)^5], \quad (18b)$$

since

$$\int_0^\infty \xi [\bar{K}_2(\xi)]^2 d\xi = \frac{2}{5}$$

(see below). Assuming α_0 independent of ϵ , and keeping only the lowest-order term in (α^2/β^2) in (18b), the total cross section is

$$\sigma_g(E) = (4096\pi/35) [A_0^2 \alpha_0^2 / (\Delta\epsilon_0)^3] (mE/M\Delta\epsilon_0)^4, \quad (18c)$$

where $\Delta\epsilon_0$ is the "average" ionization potential of the $1s\sigma_g$ MO. As we shall see, however, this result is incorrect.

2. For Coulomb trajectories

$$P_g(E, \epsilon; b) = 64A_0^2 e^{-2\omega} [\alpha^2 \beta^2 / (\alpha^2 + \beta^2)^4] S(\omega, x; \xi), \quad (19a)$$

where

$$S(\omega, x; \xi) = [\bar{K}_2(\xi) + (\frac{1}{2}\omega)(1+x^2)\bar{K}_1(\xi)]^2.$$

This gives the differential cross section

$$\sigma_g(E; \epsilon) = 128\pi A_0^2 e^{-2\omega} [\alpha^2 \beta^2 / (\alpha^2 + \beta^2)^5] I_g(\omega, x), \quad (19b)$$

where

$$I_g(\omega, x) = \int_{\xi_0}^\infty S(\omega, x; \xi) \xi d\xi, \quad \xi_0 = \omega(1+x^2)^{1/2}.$$

Now,¹⁶

$$\int_{\xi_0}^\infty \bar{K}_n(\xi) \bar{K}_m(\xi) \xi d\xi = [1/2(m+n+1)] [4\bar{K}_{n+1}(\xi_0) \bar{K}_{m+1}(\xi_0) - \xi_0^2 \bar{K}_n(\xi_0) \bar{K}_m(\xi_0)]$$

and hence $I_g(\omega, x)$ can be evaluated in closed form

$$I_g(\omega, x) = \left(\frac{2}{5}\right) \bar{K}_3^2(\xi_0) + (1+x^2) \left[\omega - \frac{1}{10} \omega^2 + \omega^2(1+x^2)/6 \right] \bar{K}_2^2(\xi_0) - [\omega^4(1+x^2)^3/24] \bar{K}_1^2(\xi_0). \quad (19c)$$

Figure 1 shows $I_g(\omega, x)$ versus x for representative values of ω . The exponential decay of the Bessel functions dominates for large $\xi_0 = \omega(1+x^2)^{1/2}$, but for the region of E, ϵ of interest to us, relevant values of x lie between 4 and 10. (For $\xi_0 \rightarrow 0, \bar{K}_3 \rightarrow 1, \bar{K}_2$ and $\bar{K}_1 \rightarrow 0.5$.) A moderate ω dependence is found in this region, but the important qualitative result is that $I_g(\omega, x)$ is roughly linear in x^2 . Taking then $I_g = I_g^0(\omega)x^2$ and keeping only the lowest-order terms in α^2/β^2 , we have

$$\sigma_g(E; \epsilon) \approx 128\pi A_0^2 I_g^0(\omega) e^{-2\omega} \beta^{-6} \quad (19d)$$

and

$$\sigma_g(E) = \left[\frac{1}{5}(2^{10}\pi I_g^0)\right] e^{-2\omega} (A_0^2/\Delta\epsilon_0^2) (mE/M\Delta G_0)^3. \quad (19e)$$

With I_g^0 taken about 0.04, and $\Delta_0 = 1.5$ a.u., σ_g agrees well with the value 5.3×10^{-6} a.u. obtained from data in Ref. 6 for $E=500$ eV. As E increases, of course, the straight-line trajectory result will eventually be recovered; this corresponds to the domain near the origin in Fig. 1 where $I_g(\omega, x)$ is flat and equal to $\frac{2}{5}$. The surprisingly large effect of the Coulomb trajectory can be rationalized if we note that due to exponential damping of $K_n(\xi)$, important contributions to $\sigma(E; \epsilon)$ all come from small impact parameters, $b < \beta^{-1} \ll \alpha^{-1} \approx a_0$.

While it is not clear how the more complicated expressions for the σ_u case will behave in detail, a power law similar to (19e) also emerges. However, both in such a result and in (19e), dependence on $\Delta\epsilon_0$ appears not only in $(mE/M\Delta\epsilon_0)^3$ but also in the coefficient in front of it. Empirically [as represented in Eq. (1)],³ both the $1s\sigma_g$ and $2p\sigma_u$ ionization cross sections are a common function of $(mE/M\Delta\epsilon_0)$. From the derivations given here, we can conclude that the slope (E dependence) of both

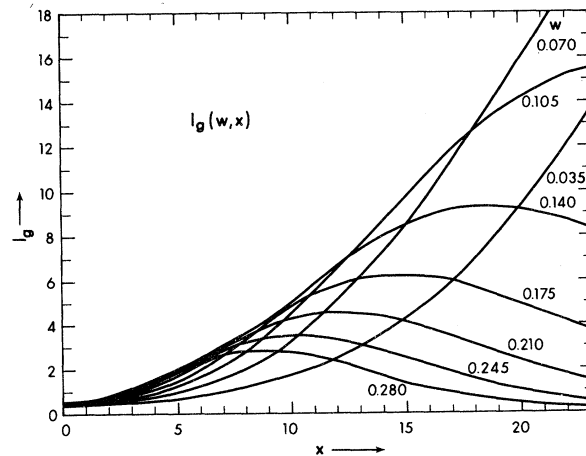


FIG. 1. Function $I_g(\omega, x)$ vs x for representative values of ω [cf. Eq. (19c)].

cross sections is the same, i.e., both depend on $(mE/M\Delta\epsilon_0)^3$; but we cannot show that the respective fore-coefficients (which in each case depend on $\Delta\epsilon_0$, amplitudes A , etc.) need be equal. The fact that they *are* so (within an order of magnitude)³ appears to be fortuitous.

The quantity $P(E; b)$ [integral of $P(E, \epsilon; b)$ over all electron energies for given impact parameter] is of some interest in connection with frequency distribution of MO x-ray emission. Figure 2 shows $\log_{10} P(E, b)$ vs b for the σ_g case, using $\alpha_0 = \text{const} = 1.5$, $\Delta\epsilon_0 = 1.5$. Note how strongly this quantity depends on the collision energy. Provided b is scaled as Z^{-1} and V as Z^{+1} , the above function is Z invariant.

C. More accurate calculations

For comparison with the results computed in Ref. 6, we have computed total cross sections $\sigma(E)$ and differential cross sections $\sigma(E; \epsilon)$, using Eqs. (12)–(16).

In the evaluation of the trajectory integrals, $\Delta\epsilon = \epsilon - \epsilon_i(R)$ is assumed to have a constant "average" value. This is certainly not valid in the *gerade* case, since the MO ionization potential $-\epsilon_{1s\sigma_g}(R)$ varies from 2.0 a.u. at $R=0$ to 0.5 a.u. at

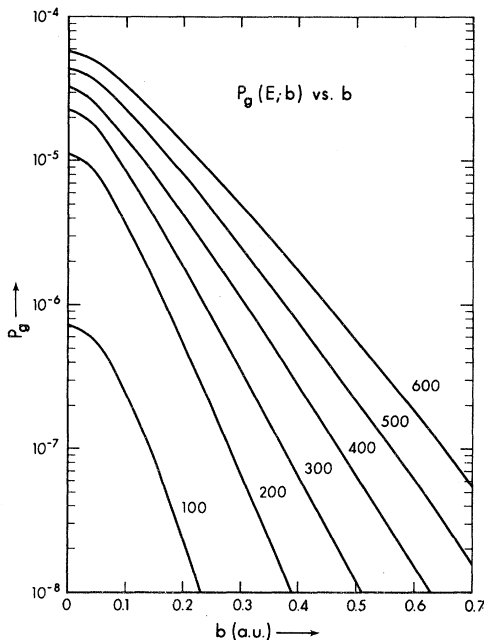


FIG. 2. Ionization probability function $P_g(E, b)$ vs b for various values of E . Note the pronounced velocity dependence of the profile. If b is scaled as Z^{-1} and V as Z^{+1} , P_g is Z invariant (note that c.m. energies E are those for H_2^+ , not D_2^+). Above curves based on Eq. (19a), with $\alpha_0 = \text{const} = 1.5$; $\Delta\epsilon_0 = \text{const} = 1.5$.

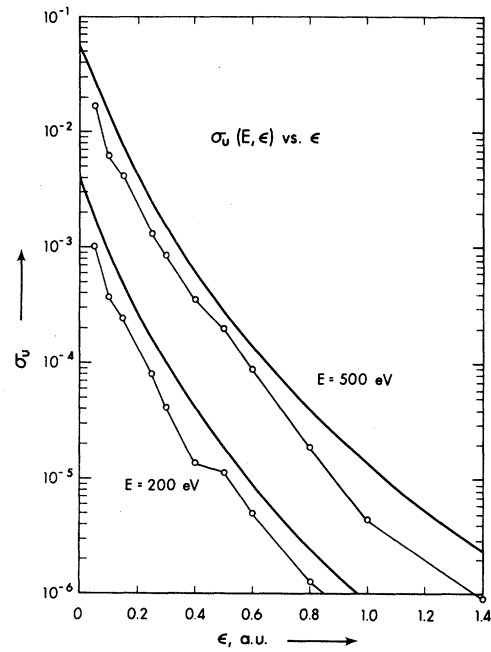


FIG. 3. Differential ungerade cross sections $\sigma_u(E, \epsilon)$ vs ejected electron energy ϵ , at $E=500$ and 200 eV. Solid curves, model calculation (correction factor $C_0=1$); open circles, "exact" calculations of Ref. 6.

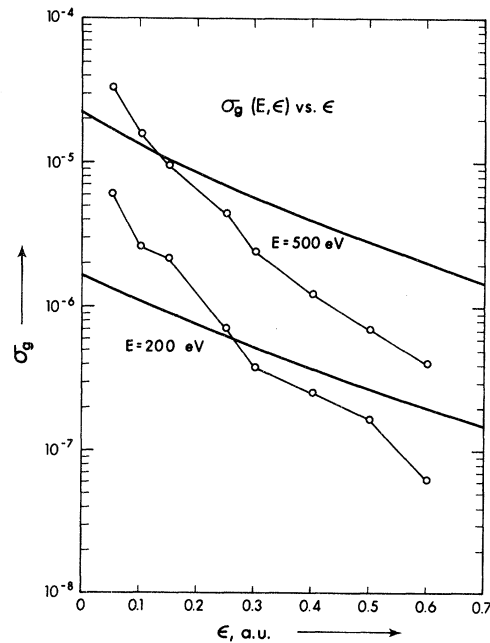


FIG. 4. Differential gerade cross sections $\sigma_g(E, \epsilon)$ vs ϵ , at $E=500$ and 200 eV. Solid curves, model calculations with $C_0=0.75$; open circles, "exact" calculations of Ref. 6.

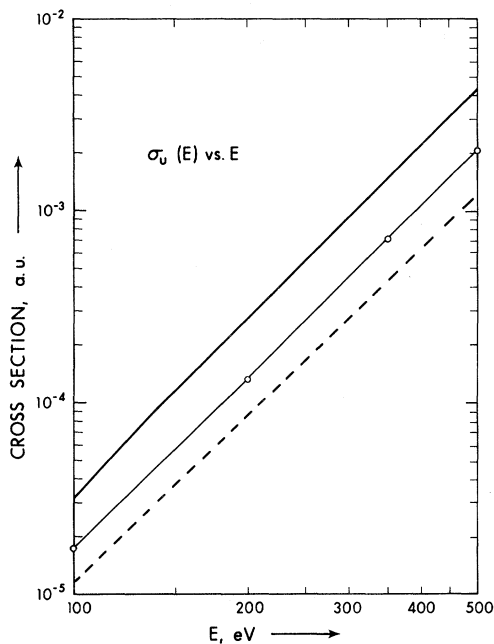


FIG. 5. Total ungerade cross sections $\sigma_u(E)$ vs E . Open circles, "exact" calculations; solid curve, present model $\sigma_u(E)$; dashed curve, comparison " $\sigma_g(E)$ " obtained using $2p\sigma_u$ ionization potential but $1s\sigma_g$ matrix elements.

$R \rightarrow \infty$; in the $2p\sigma_u$ case it is more nearly valid, the ionization potential being close to 0.5 a.u. at all R . Since the magnitude of the trajectory integral at a given impact parameter depends exponentially on $\Delta\epsilon$, we must take an appropriate choice for the "average" value used. If we wish, this can be considered a function of b (even though constant in the trajectory integral), though in fact we find that such variation has little effect on the results, since most of the cross section comes from collisions with small $b \lesssim (v/\Delta\epsilon_0)$. We used

$$\Delta\epsilon_i(E, \epsilon; b) = \epsilon - C_0\epsilon_i[R_0(E, b)], \quad (20)$$

where R_0 is the closest approach distance for that b , E , $\epsilon_i(R)$ is the exact H_2^+ MO energy, and C_0 is an adjustable "correction factor." For the $1s\sigma_g$ case, where $-\epsilon_{1s\sigma_g}(R)$ decreases with increasing R , C_0 should be less than 1. However, even introducing this correction cannot compensate for the error introduced by assuming $\Delta\epsilon$ constant in the integrals.

This expectation is borne out by the comparisons shown in Figs. 3 and 4 between the calculations of $\sigma(E, \epsilon)$ given by Ref. 6 and those of the model used here. For the σ_u case we took $C_0 = 1.0$ and the general agreement with the slopes for the exact calculations is quite good (in view of other approximations made in calculating the u model cross sec-

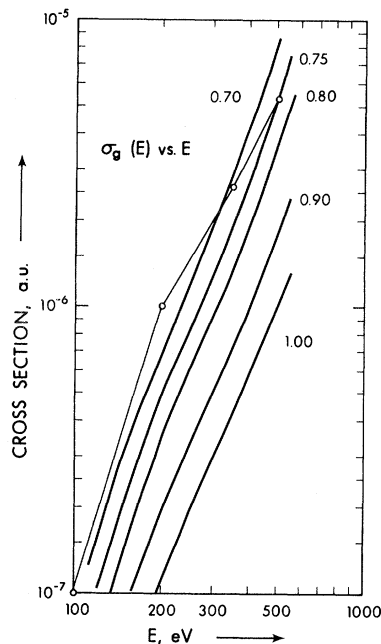


FIG. 6. Total gerade cross sections $\sigma_g(E)$ vs E . Open circles, calculations from Ref. 6; solid curves, model calculations for various values of correction factor C_0 .

tions we did not consider adjustment of C_0 to get agreement of magnitudes to be relevant). On the other hand, in the σ_g case it is clear that the model curves have slopes much less than those for the exact calculations.

Figures 5 and 6 compare model calculations of $\sigma_u(E)$ and $\sigma_g(E)$ versus E , with those of Ref. 6 [$\sigma_g(E)$ was not reported in Ref. 6; the values are 1×10^{-7} , 1.0×10^{-6} , 2.6×10^{-6} , and 5.3×10^{-6} a.u. at 100, 200, 350, and 500 eV, respectively]. Considering the approximations made in the model, agreement in magnitude and especially in slope between exact and model results is extremely good for the σ_u case; indeed, the model curve $\sim E^{2.93}$, while the "exact" curve $\sim E^{2.98}$, both in good agreement with the crude law (19e). In order to indicate how closely the σ_g cross-section magnitude would compare with that of σ_u if their ionization potentials were comparable, we ran a model calculation for $1s\sigma_g$ using $\Delta\epsilon$ values taken from the $2p\sigma_u$ MO but integrals for the $1s\sigma_g$ case; the result is shown by the dashed line in Fig. 5. For the $1s\sigma_g$ case agreement between model and "exact" calculations is less satisfactory. Model curves for various choices of C_0 are shown, with values for C_0 between 0.70 and 0.80 best approximating the data. We believe that precision errors in the calculations of $\sigma_g(E)$ based on Ref. 6 are too large

to decide whether or not the slopes are in reasonable agreement with the model or not. The peculiar reversing curvature of the model curves in Fig. 6 shows the trend to the fourth-power law (18c) at higher energies ($E > 500$ eV), and to an exponential decay due to the Bessel function cutoff in (19c) as E decreases (ω, x increase).

The scaled experimental data presented by Meyerhof and co-workers¹⁻³ have a persistently greater slope [$\ln\sigma(E)$ versus $\ln E$] than the value of 3 predicted by this model. While we cannot say with certainty that the Ref. 6 calculations for $\sigma_g(E)$ do or do not agree with the model, it seems evident that in the $2p\sigma_u$ case the model has accounted essentially quantitatively for the results for H_2^+ from Ref. 6. Differences observed for the heavy ions for $2p\sigma_u$ should therefore presumably be attributed to effects of the other electrons on the ionization process. Since there is a large remaining uncertainty in the $1s\sigma_g$ case, both as to the true slope of the Ref. 6 cross section and as to the effect of assuming $\epsilon_{1s\sigma_g}(R)$ constant, as the model does, we cannot decide whether the steeper slope observed for $1s\sigma_g$ vacancy production in heavy ions does or does not agree well with the H_2^+ -system behavior.

In any case, however, it is evident that the energy dependence of these ionization cross sections is essentially completely determined by the oscillatory factor arising from transfer of momentum/energy from the heavy particles to the electron, and is independent of the type of electronic coupling matrix elements; furthermore, the large difference in magnitude between $1s\sigma_g$ and $2p\sigma_u$ cross sections is also due to the effect of changes in $\Delta\epsilon$ on the frequency of the oscillatory factor; within

about an order of magnitude the variations in shape and size of the various radial and rotational coupling elements have little effect on the cross sections.

D. Precision errors in the results of Ref. 6

There are evidently significant precision errors in the calculations of Ref. 6. Experience gained in the model calculations suggests that the source of these errors lies in our inability to economically and accurately fit the matrix elements to smooth analytical forms.

All trajectory integrals and associated ionization probabilities $P(E, \epsilon, b)$ obtained in model calculations are found to be smooth nonoscillatory functions of b , but typical plots of $P(E, \epsilon, b)$ obtained in Ref. 6 always had rapid fluctuations. We conclude this is "noise" generated by very small but nonzero discontinuities between successive overlapping rational polynomial "fits" to the matrix elements. Unfortunately, to use elaborate smooth analytical fits to the matrix elements valid over the whole range of quadrature would have been prohibitively expensive.

ACKNOWLEDGMENTS

I thank Dr. W. E. Meyerhof of Stanford University for stimulating this study by his interesting experimental work, and for helpful discussions and private correspondence on the problem. Computations were performed at the University of Alberta Computing Centre. Part of this work was done while I was a sabbatical visitor (1974) at the Theoretical Chemistry Department, Oxford University, to whom I am obliged for their great hospitality.

*Work supported by the National Research Council of Canada.

¹W. E. Meyerhof, Phys. Rev. A **10**, 1005 (1974). Unfortunately, the results of Refs. 6 and 11 were incorrectly plotted in the above paper; all energies E are double those plotted [W. E. Meyerhof (private communication)]. When correctly plotted the scaled theoretical ionization cross sections are about an order of magnitude smaller than experimental vacancy-production cross sections.

²W. E. Meyerhof, T. K. Saylor, S. M. Lazarus, A. Little, B. B. Triplett, L. F. Chase, Jr., and R. Anholt, Phys. Rev. Lett. **32**, 1279 (1974).

³W. E. Meyerhof, R. Anholt, T. K. Saylor, and P. D. Bond, in *Fourth International Conference on Atomic Physics, Heidelberg, Abstracts of Contributed Papers*, edited by J. Kowalski and H. G. Weber (Springer-Verlag, Heidelberg, 1974), p. 625; Phys. Rev. A (to be

published) (see note in Ref. 1).

⁴W. R. Thorson and H. Levy II, Phys. Rev. **181**, 230 (1969); H. Levy II and W. R. Thorson, *ibid.* **181**, 244 (1969); **181**, 252 (1969).

⁵C. F. Lebeda, W. R. Thorson, and H. Levy II, Phys. Rev. A **4**, 900 (1971).

⁶V. Sethuraman, W. R. Thorson, and C. F. Lebeda, Phys. Rev. A **8**, 1316 (1973).

⁷W. R. Thorson (unpublished); cf. also J. S. Briggs and J. Macek, J. Phys. B **5**, 579 (1972); **6**, 982 (1973).

⁸W. E. Meyerhof (private communications); S. S. Hanna and W. E. Meyerhof (unpublished); W. E. Meyerhof, T. K. Saylor, S. M. Lazarus, A. Little, R. Anholt, and L. F. Chase, Jr. (unpublished).

⁹V. Fano and W. Lichten, Phys. Rev. Lett. **14**, 627 (1965); M. Barat and W. Lichten, Phys. Rev. A **6**, 211 (1972); W. E. Meyerhof, Phys. Rev. Lett. **31**, 1341 (1973).

- ¹⁰W. E. Meyerhof, in *Third International Seminar on Ion-Atom Collisions*, Gif-sur-Yvette, France, 1973 (unpublished); the same idea has been suggested by C. Foster, T. Hoogkamer, and F. W. Saris [J. Phys. B 7, 2563 (1974)]; B. Fastrup, E. Bøving, G. A. Larsen, and P. Dahl [*ibid.* 7, L206 (1974)]; M. C. Chidimio-Frank and R. D. Piacentini [*ibid.* 7, 548 (1974)].
- ¹¹S. K. Knudson and W. R. Thorson, Can. J. Phys. 48, 313 (1970).
- ¹²Plots of angular matrix elements given in Refs. 4-6 actually show the matrix elements divided by R^2 .
- ¹³I. S. Gradshteyn and I. M. Ryzhik, in *Table of Integrals, Series, and Products*, 4th ed., edited by A. Jeffrey (Academic, New York, 1965), Formulas 3.961.1 and 3.961.2. I thank W. E. Meyerhof for drawing my attention to these formulas, which are equivalent to but much simpler than a more easily derived infinite-series expansion in $K_n(\xi)$.
- ¹⁴The asymptotic expansion is obtained by expanding the Gaussian in its Taylor series on the real axis, then performing the integral for each term on a contour on the upper right-hand quarter-circle at ∞ , down the positive imaginary axis from ∞ to $+1$, around the branch line at $+i$, then back up the imaginary axis to ∞ and around the upper left-hand quarter-circle to the negative real axis. Since the Gaussian diverges on the infinite quarter-circles such a procedure cannot be truly convergent, but it can be shown that when $x = \xi/\tau$ is large enough the expansion is a useful asymptotic approximation.
- ¹⁵Strictly speaking, M scales with Z^{+1} if we use the mass for D rather than for H in performing calculations. This would mean employing ω values half as large as those we actually used. We wished in the first instance to compare these model calculations with those of Ref. 6, so we employed H_2^+ parameters. However, we found that even halving ω as required for a good scaling makes no great difference to the cross sections, because the cross section depends only weakly on ω in the relevant energy region.
- ¹⁶M. Abramowitz and I. Stegun, *Handbook of Mathematical Functions*, Natl. Bur. Std. Appl. Math. Series No. 55 (U. S. GPO, Washington, D. C., 1964), Formulas 11.3.31 (p. 484) and 9.6.26 (p. 376).